Chen et al. *Zool. Res.* 2024, 45(5): 1108−1115
https://doi.org/10.24272/j.issn.2095-8137.2024.186
https://cstr.cn/32248.14.zr.2024.186

ZR | Zoological Research

Article Open Access

Overexpression of *Kdm6b* induces testicular differentiation in a temperature-dependent sex determination system

Qiran Chen[1,2,#], Wei Sun[1,2,#], Lin Jin[1,2], Yingjie Zhou[1,2], Fang Li[1,2], Chutian Ge[1,2,*]

[1] *College of Biological and Environmental Sciences*, *Zhejiang Wanli University*, *Ningbo*, *Zhejiang* 315100, *China*
[2] *Institute of Animal Sex and Development*, *Zhejiang Wanli University*, *Ningbo*, *Zhejiang* 315100, *China*

ABSTRACT

In reptiles, such as the red-eared slider turtle (*Trachemys scripta elegans*), gonadal sex determination is highly dependent on the environmental temperature during embryonic stages. This complex process, which leads to differentiation into either testes or ovaries, is governed by the finely tuned expression of upstream genes, notably the testis-promoting gene *Dmrt1* and the ovary-promoting gene *Foxl2*. Recent studies have identified epigenetic regulation as a crucial factor in testis development, with the H3K27me3 demethylase KDM6B being essential for *Dmrt1* expression in *T. s. elegans*. However, whether KDM6B alone can induce testicular differentiation remains unclear. In this study, we found that overexpression of *Kdm6b* in *T. s. elegans* embryos induced the male development pathway, accompanied by a rapid increase in the gonadal expression of *Dmrt1* at 31°C, a temperature typically resulting in female development. Notably, this sex reversal could be entirely rescued by *Dmrt1* knockdown. These findings demonstrate that *Kdm6b* is sufficient for commitment to the male pathway, underscoring its role as a critical epigenetic regulator in the sex determination of the red-eared slider turtle.

Keywords: Temperature-dependent sex determination; Sex reversal; *Kdm6b*; *Dmrt1*; *T. s. elegans*

INTRODUCTION

Temperature-dependent sex determination (TSD) is an evolutionary adaptation observed in many reptiles (Schwanz & Georges, 2021; Warner & Shine, 2008). Unlike genotypic sex determination (GSD), where sex is predetermined by robust genetic forces (e.g., *Sry* in mammals and *Dmrt1* in birds) on sex chromosomes, TSD relies on environmental temperatures during embryonic development to establish primary gonadal sex (Kashimada & Koopman, 2010; Koopman et al., 1991; Smith et al., 2009; Weber & Capel, 2021). Despite the fundamental disparity in initiation, the key genes involved in testicular (*Dmrt1*, *Sox9*, and *Amh*) and ovarian (*Foxl2* and *Cyp19a1*) differentiation are remarkably conserved across both TSD and GSD species (Bertho et al., 2016; Cutting et al., 2013; Hui et al., 2021; Ma et al., 2022; Vining et al., 2021; Weber & Capel, 2021). As genomes are identical between males and females in TSD species due to the absence of sex chromosomes (Weber & Capel, 2021), it is plausible that sex determination is mediated through the regulation of these conserved genes, likely via epigenetic mechanisms.

Epigenetic regulation, encompassing processes such as DNA methylation and histone modification, alters gene expression without modifying the DNA sequence itself. By modifying the chemical tags on DNA or histones, it can activate, repress, or sustain the expression of specific target genes (Kuroki & Tachibana, 2018; Reik, 2007; Wei & Wu, 2022). Recent evidence has shed light on the pivotal role of epigenetic modifiers in shaping sexual differentiation in both GSD and TSD species by regulating the expression of key sex-determining factors (Ge et al., 2018; Kuroki & Tachibana, 2018). In mice, KDM3A (also known as JMJD1A) has been identified as a critical regulator that modulates the expression of the Y chromosome sex-determining gene *Sry* through the demethylation of H3K9me2 in XY individuals (Kuroki et al., 2013). Moreover, chromodomain Y-like protein (CDYL) and the polycomb repressive complex 1 subunit CBX2 maintain H3K27me3 levels on the *Wnt4* and *Lef1* promoters, respectively, thereby repressing female pathways (Garcia-Moreno et al., 2019; Katoh-Fukui et al., 2012; Okashita et al., 2023). Furthermore, sexually dimorphic DNA methylation patterns in the promoters of genes such as *Dmrt1* and *Cyp19a1*, observed in various species, including reptiles and fish, can be influenced by environmental factors, particularly temperature, and may even be heritable (Ge et al., 2017; Matsumoto et al., 2013; Shao et al., 2014; Wang et al., 2022).

The red-eared slider turtle (*Trachemys scripta elegans*) is

Received: 22 July 2024; Accepted: 12 August 2024; Online: 13 August 2024

Foundation items: This work was supported by the National Natural Science Foundation of China (32325049, U22A20529, 32303000), Zhejiang Provincial Natural Science Foundation (LQ24C190009), Ningbo Natural Science Foundation (2022J192), and Zhejiang Provincial Top Key Discipline of Biological Engineering (1741000592)

[#]Authors contributed equally to this work

*Corresponding author, E-mail: cge@zwu.edu.cn

one of the most comprehensively studied TSD species. During the thermosensitive period (TSP) of embryogenesis, spanning stages 15 to 19, this species produces exclusively female or male offspring depending on the incubation temperature, with high temperature (31°C) producing females (FPT) and low temperature (26°C) producing males (MPT) (Bull & Vogt, 1979; Wibbels et al., 1991). A recent breakthrough has been achieved with the discovery of the epigenetic regulation of *Dmrt1* by KDM6B (JMJD3), a histone demethylase of H3K27me3. Notably, in KDM6B-knockdown (KD) gonads, the suppression of male sex-determining genes results in the development of ovaries even at MPT (Ge et al., 2018). However, whether *Kdm6b* overexpression (OE) is sufficient to drive male development at FPT remains unclear.

In this study, we found that overexpression of the KDM6B open reading frame (ORF) successfully induced *Dmrt1* expression and promoted testicular development in the gonads of red-eared slider turtles under FPT conditions. Moreover, this induced sex reversal was rescued by *Dmrt1* knockdown following *Kdm6b* overexpression. These results provide compelling evidence that KDM6B acts as a master epigenetic regulator, sufficient to drive testis development through the up-regulation of *Dmrt1* expression in the sex determination process of *T. s. elegans*.

MATERIALS AND METHODS

Experimental animals

Freshly laid *T. s. elegans* eggs were obtained from the Hanshou Institute of Turtles (Hunan, China). Fertilized eggs were promptly collected and placed in an incubator at either 26°C or 31°C, with humidity maintained at 70%–80%. Embryonic developmental stages were determined according to previously established criteria (Greenbaum & Carr, 2002). Gonads were harvested from embryos at stages 16, 17, 21, and 25 across various experimental groups, washed in phosphate-buffered saline (PBS, Sangon, China), and submerged in Trizol reagent (Invitrogen, USA) for RNA extraction. Gonad-mesonephros complexes at stages 21 and 25 were fixed in 4% paraformaldehyde (PFA, Macklin, China) for immunofluorescence analysis.

Constructs of *Kdm6b* overexpression lentiviral vectors

The lentiviral vector for overexpressing turtle *Kdm6b* was prepared according to our previous report (Ma et al., 2022). Briefly, the full-length turtle *Kdm6b* ORF was amplified from testis cDNA and subsequently inserted into the pGLV-EF1a-GFP vector (LV-4, GenePharma, China). The resulting recombinant construct pGLV-EF1a-GFP-*Kdm6b* was named LV-*Kdm6b*-OE. The pGLV-GFP-empty vector (LV-empty) was employed to serve as a negative control. Lentivirus production was carried out as described in our previous study (Ma et al., 2022). HEK293T cells were transfected with the constructed lentiviral vectors alongside packaging plasmids (pGag/Pol, pRev, and pVSV-G). After 24 h of culture at 37°C, the lentivirus was harvested via centrifugation at 4 000 ×*g* for 15 min at 4°C and filtered using a 0.45 μm filter (Millipore, USA). A viral titer of 4×10^8 infectious units/mL was obtained.

Constructs of *Dmrt1* shRNA lentiviral vectors

Lentivector-*Dmrt1*-shRNA constructs were prepared followed previously reported methods (Ge et al., 2017). In brief, a shRNA sequence (5′-GGTGGCAGCTCCTGTTTATTG-3′) with demonstrated high efficiency (Ge et al., 2017) was selected, synthesized, and inserted into a pGP-U6 vector (GenePharma, China) to generate pGP-U6-*Dmrt1*-shRNA. The resulting construct was then digested with AgeI-EcoRI and subcloned into the EcoRI site of the pGLV-U6-GFP vector (GenePharma, China), producing the recombinant construct pGLV-U6-GFP-*Dmrt1*-shRNA, designated LV-*Dmrt1*-KD. A negative control vector (pGLV-GFP-NC-shRNA, designated LV-NC-shRNA) was also prepared. High-quality proviral DNA was subsequently prepared for transfection into HEK293T cells using Lipofectamine 2000 (Invitrogen, USA). The viral titer reached 4×10^8 infectious units/mL, with the viral particles then stored at −80°C until further examination.

Infection of turtle embryos

Turtle eggs were sterilized by swabbing with alcohol pads. High-titer LV-*Kdm6b*-OE virus was injected into stage 15 turtle embryos at FPT (31°C), either alone or in combination with the LV-*Dmrt1*-shRNA virus using a Hamilton needle. Approximately 5 μL of the virus solution was injected per embryo, with a total of 400 eggs injected in each treatment group. Control embryos at FPT and MPT were injected with LV-empty virus (200 embryos each). Eggs were sealed with parafilm and incubated at 31°C. Embryos showing GFP fluorescence were collected for further examination.

Quantitative real-time polymerase chain reaction (qPCR)

For the qPCR experiments, 0.5–2.0 μg of total RNA was treated by DNase I (Thermo Fisher Scientific, USA) and reverse-transcribed using a RevertAid™ First Strand cDNA Synthesis Kit (Thermo Fisher Scientific, USA) according to the manufacturer's instructions. The qPCR procedures were performed in triplicate with a 2X Universal SYBR Green Fast qPCR Mix (ABclonal, China) on a Bio-Rad iCycler system (Bio-Rad, USA). After normalization with *Gapdh*, relative mRNA levels were calculated using the $2^{-\Delta\Delta Ct}$ method. The primer sequences for qPCR are listed in Supplementary Table S1.

Hematoxylin-eosin (H&E) staining

Gonad-mesonephros complexes were fixed in 4% PFA overnight at 4°C, then embedded in paraffin wax and transversely sectioned into 6 μm slices. The paraffin sections were deparaffinized and rehydrated before H&E staining. The stained sections were visualized under light microscopy (Nikon, Japan).

Immunofluorescence staining

Staining was carried out as reported previously (Tezak et al., 2023). In brief, 6-μm-thick gonadal slices were rehydrated and subjected to 10 mmol/L sodium citrate (Sangon, China) buffer at 96°C for antigen retrieval. After rinsing with PBS containing 0.3% Triton X-100 (PBST), the sections were blocked and incubated overnight at 4°C with primary antibodies, including rabbit anti-SOX9 (Chemicon, AB5535, 1:1 000, USA), goat anti-FOXL2 (HUABIO, 1:300, China), mouse anti-CYP19A1 (HUABIO, 1:300, China), mouse anti-β-catenin (Sigma, C7207, 1:250, USA), rabbit anti-AMH (HUABIO, 1:500, China), and rabbit anti-VASA (Abcam, ab13840, 1:500, USA). Signals were detected using secondary antibodies Alexa Fluor 488 donkey anti-mouse IgG (Invitrogen, A21202, USA) and Alexa Fluor 594 donkey anti-rabbit IgG (Invitrogen, A21207, USA), diluted at 1:250. Nuclei were stained with 4',6-diamidino-2-phenylindole (DAPI, Sigma, D9542, USA). Photomicrographs were captured using a confocal microscope (A1 Plus, Nikon, Japan).

Statistical analyses

Statistical analyses were performed using GraphPad Prism v.8 (Dotmatics, USA). Statistical significance between groups was analyzed using an unpaired Student's *t*-test (*: P<0.05; **: P<0.01; ***: P<0.001; ns: Not significant). All data are shown as mean±standard deviation (SD) (n=3).

RESULTS

Overexpression of *Kdm6b* induces masculinization of FPT gonads *in vivo*

To elucidate the role of *Kdm6b* in initiating the male developmental pathway, lentiviral vectors carrying the *Kdm6b* ORF were introduced into red-eared slider turtle eggs at FPT during the early stage of sex determination (stage 15). The qPCR results revealed a rapid increase in the expression of *Kdm6b* at stage 16, which continued to rise through stage 17, reaching levels comparable to those observed in non-silencing control MPT gonads, confirming efficient lentiviral transduction (Supplementary Figure S1).

Phenotypic analysis showed that control FPT embryos exhibited typical female characteristics, including elongated and flattened gonads and the presence of oviducts on the mesonephros. In contrast, control MPT embryos displayed short, thick gonads with no oviducts on the mesonephros. Furthermore, FPT embryos overexpressing *Kdm6b* exhibited a transformation in gonadal morphology, shifting from flat to rounded, closely resembling that of male gonads, despite no significant change in gonadal length (Figure 1A). Histological analysis demonstrated varying degrees of sex reversal in FPT embryos overexpressing *Kdm6b*, ranging from complete sex reversal (47 out of 59 embryos, Table 1), marked by cortical tissue degeneration, well-defined medulla, and seminiferous cord formation, to partial reversal (11 out of 59 embryos, Table 1), marked by the coexistence of both cortical and seminiferous cord tissues within their gonads (Figure 1B). Furthermore, analysis of germ cell distribution indicated that VASA-positive germ cells were predominantly localized in the cortical region of control FPT gonads, whereas they were confined to the medullary cords in control MPT gonads. In gonads infected with *Kdm6b*-OE lentiviral vectors, most germ cells successfully completed migration and were arrested within the seminiferous cords (Figure 1C).

The expression levels of markers associated with testicular

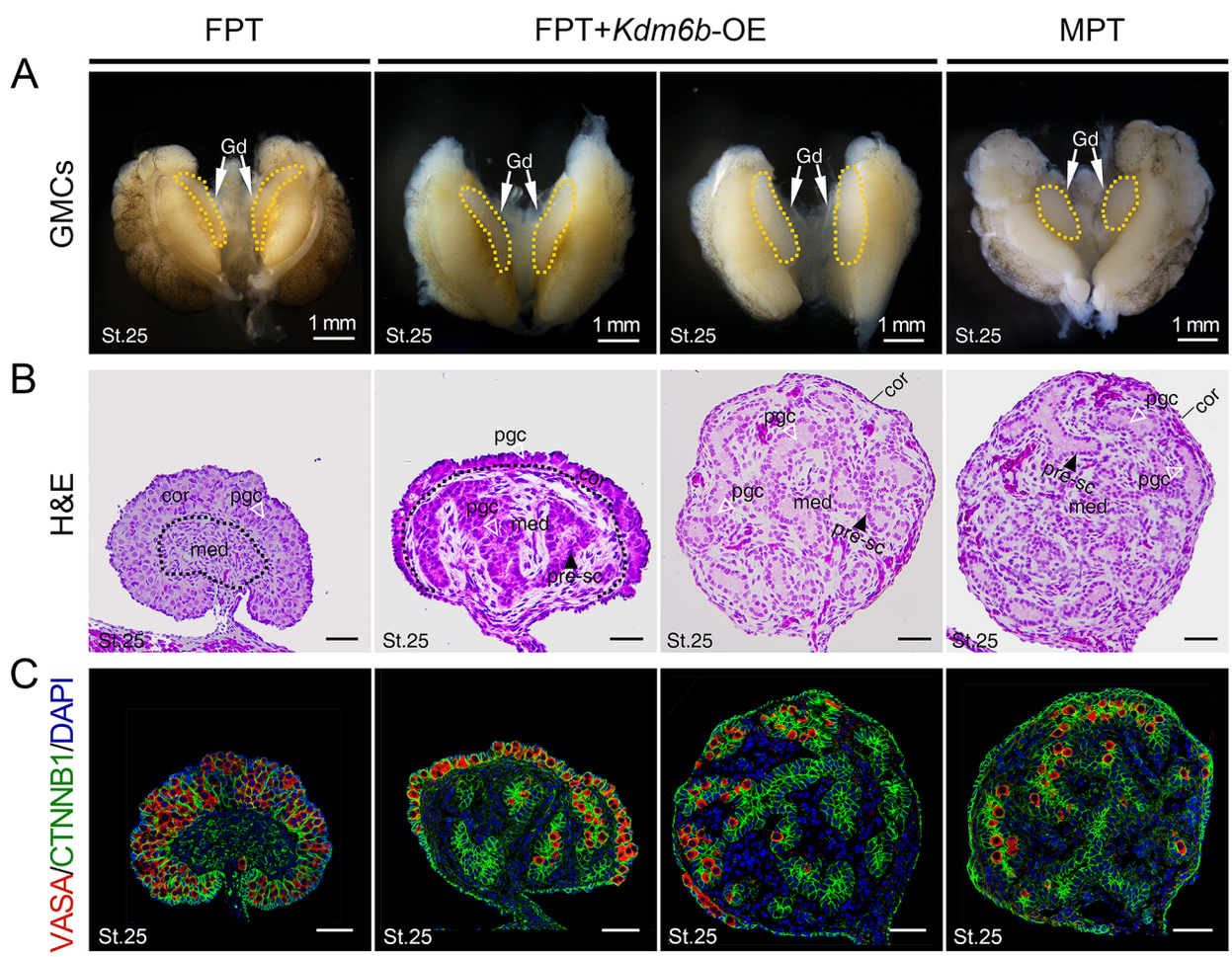

Figure 1 Morphological assessment of FPT gonads overexpressing *Kdm6b*

A: Representative images of gonad-mesonephros complexes from FPT, FPT+*Kdm6b*-OE, and MPT embryos at stage 25. Gonads are outlined by yellow dotted lines. B: Hematoxylin and eosin (H&E) staining of gonadal sections from FPT, FPT+*Kdm6b*-OE, and MPT embryos at stage 25. Boundary between cortical and medullary regions is denoted by black dotted lines. Gd, gonad; sc, seminiferous cord; pgc, primordial germ cells; cor, cortex; med, medulla. C: Expression profiles of VASA and CTNNB1 proteins in gonadal sections from control FPT, FPT+*Kdm6b*-OE, and control MPT embryos at stage 25. Most VASA-positive germ cells successfully migrated to seminiferous cords in *Kdm6b*-OE FPT gonads. Scale bars: 50 μm.

(*Sox9* and *Amh*) and ovarian (*Foxl2* and *Cyp19a1*) differentiation were subsequently analyzed in *Kdm6b*-OE gonads. In comparison to control FPT gonads, the *Kdm6b*-OE gonads exhibited a marked increase in *Sox9* and *Amh* expression, accompanied by a significant decrease in *Foxl2* and *Cyp19a1* expression. Notably, no significant difference was observed in the expression levels of these genes compared to the control MPT group (Figure 2A).

The SOX9 protein expression pattern at stages 21 and 25 was examined using immunofluorescence. Results showed that SOX9 was localized exclusively to Sertoli cells in the control MPT gonads but was absent in the control FPT gonads. However, in the OE group, SOX9 signals were detected within the testicular cord-like structures in FPT gonads (Figure 2B). Likewise, AMH, another Sertoli cell marker, was detected in the well-developed medulla of all

Table 1 Sex ratio (percentage of testes) of *Kdm6b*-OE gonads at 31°C

Incubation temperature	Viral treatment	Embryos	Testes	Ovaries	Ovotestes	Sex ratio (% testes)
FPT (31°C)	Control	40	0	40	0	0/40
FPT (31°C)	LV-*kdm6b*-OE	59	47	1	11	(47+11)/59
MPT (26°C)	Control	40	40	0	0	40/40

Gonadal sex was determined by morphological analysis of gonads. FPT, high temperature (31°C) producing females; MPT, low temperature (26°C) producing males.

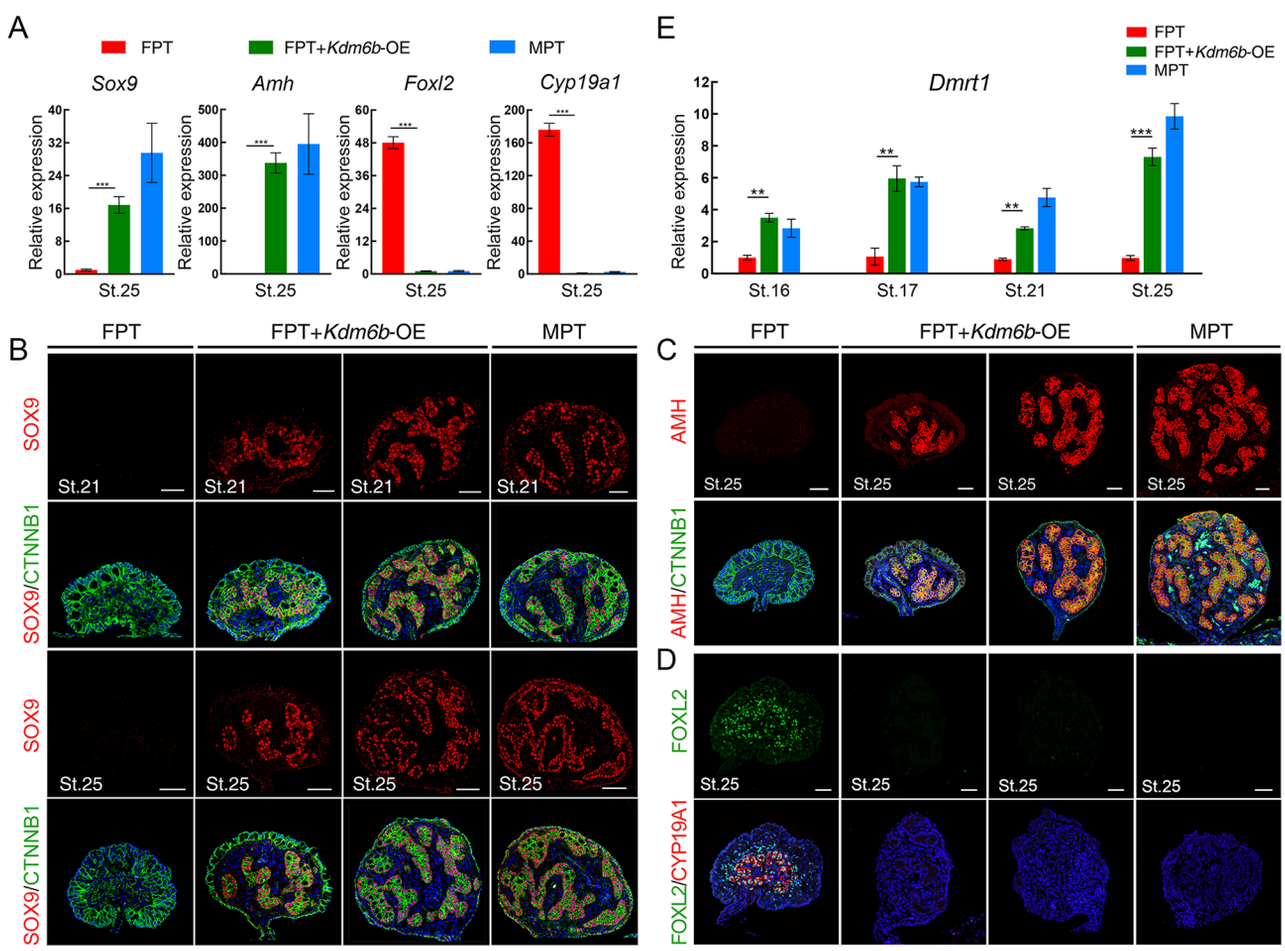

Figure 2 Expression changes in sex-specific markers in FPT gonads overexpressing *Kdm6b*

A: qPCR analysis of *Sox9*, *Amh*, *Foxl2*, and *Cyp19a1* in FPT, FPT+*Kdm6b*-OE, and MPT gonads at stage 25. Significant up-regulation of *Sox9* and *Amh*, and significant down-regulation of *Foxl2* and *Cyp19a1* were observed in *Kdm6b*-OE FPT gonads at stage 25. Relative quantification of genes was normalized to *Gapdh*. Data are presented as mean±SD; ***: $P<0.001$; $n=3$. B: Immunofluorescence analysis of SOX9 and CTNNB1 proteins counterstained with DAPI (blue) in gonadal sections from control FPT, FPT+*Kdm6b*-OE, and control MPT embryos at stages 21 and 25. SOX9 protein expression was significantly increased in *Kdm6b*-OE FPT gonads. CTNNB1 expression revealed a degenerated cortex and developing medullary cords in *Kdm6b*-OE FPT gonads. C: Immunofluorescence analysis of AMH and CTNNB1 proteins counterstained with DAPI in gonadal sections from control FPT, FPT+*Kdm6b*-OE, and control MPT embryos at stage 25. AMH protein expression was significantly up-regulated in *Kdm6b*-OE FPT gonads. D: Immunofluorescence analysis of FOXL2 and CYP19A1 proteins counterstained with DAPI in gonadal sections from control FPT, FPT+*Kdm6b*-OE, and control MPT embryos at stage 25. No expression of FOXL2 and CYP19A1 was detected in *Kdm6b*-OE FPT gonads. Scale bars: 50 μm. E: qPCR analysis of *Dmrt1* in gonads from FPT, FPT+*Kdm6b*-OE, and MPT gonads at stages 16, 17, 21, and 25. Rapid and continuous up-regulation of *Dmrt1* upon *Kdm6b* overexpression was detected. Results were normalized to *Gapdh*. Data are presented as mean±SD; **: $P<0.05$; ***: $P<0.01$. $n=3$.

samples in the OE group at stage 25 (Figure 2C). In contrast, FOXL2 and CYP19A1, predominantly expressed in pre-granulosa cells in female ovaries, were undetectable in the *Kdm6b*-OE gonads (Figure 2D). Together, these results strongly support female-to-male sex reversal in *Kdm6b*-OE gonads under FPT.

Given that *Dmrt1* is a direct target of *Kdm6b* (Ge et al., 2018), we investigated its expression in the *Kdm6b*-OE group gonads. As expected, *Dmrt1* levels increased rapidly after injection of the *Kdm6b*-OE virus and continued to rise throughout embryonic development (Figure 2E). These findings suggest that overexpression of *Kdm6b* can induce male differentiation by significantly up-regulating *Dmrt1* expression.

Knockdown of *Dmrt1* rescues the female pathway in turtles overexpressing *Kdm6b*

To determine whether *Dmrt1* knockdown can reverse the masculinization of gonads induced by *Kdm6b* overexpression, *Dmrt1*-KD lentiviral vectors were co-transduced into the *Kdm6b*-OE gonads. Despite the sustained high expression of *Kdm6b*, *Dmrt1* levels were significantly reduced (Supplementary Figure S2).

Histological analysis revealed that 94% (17/18) of gonads exhibited varying degrees of female-to-male sex reversal following *Kdm6b* overexpression. Remarkably, this sex reversal was completely rescued following *Dmrt1* knockdown (12/12) (Table 2). In all examined samples, the cortex developed normally, and no seminiferous cords were observed in the medullary region at stage 21 (Figure 3A). Furthermore, VASA-positive germ cells in these gonads, unlike in the *Kdm6b*-OE group, remained in the cortex rather than migrating to the seminiferous cords (Figure 3B).

At stage 21, compared to both the *Kdm6b*-OE and control MPT groups, the co-transduction group displayed a significant down-regulation of *Sox9* and up-regulation of *Cyp19a1*, resembling the expression levels observed in the control FPT

Table 2 Sex ratio (percentage of testes) of gonads with *Kdm6b*-OE and *Dmrt1*-KD at 31°C

Incubation temperature	Viral treatment	Embryos	Testes	Ovaries	Ovotestes	Sex ratio (% testes)
FPT (31°C)	Control	30	0	30	0	0/30
FPT (31°C)	LV-*Kdm6b*-OE	18	10	1	7	(10+7)/18
FPT (31°C)	LV-*Kdm6b*-OE +*Dmrt1*-KD	12	0	12	0	0/12
MPT (26°C)	Control	30	30	0	0	30/30

Gonadal sex was determined by morphological analysis of gonads. FPT, high temperature (31°C) producing females; MPT, low temperature (26°C) producing males.

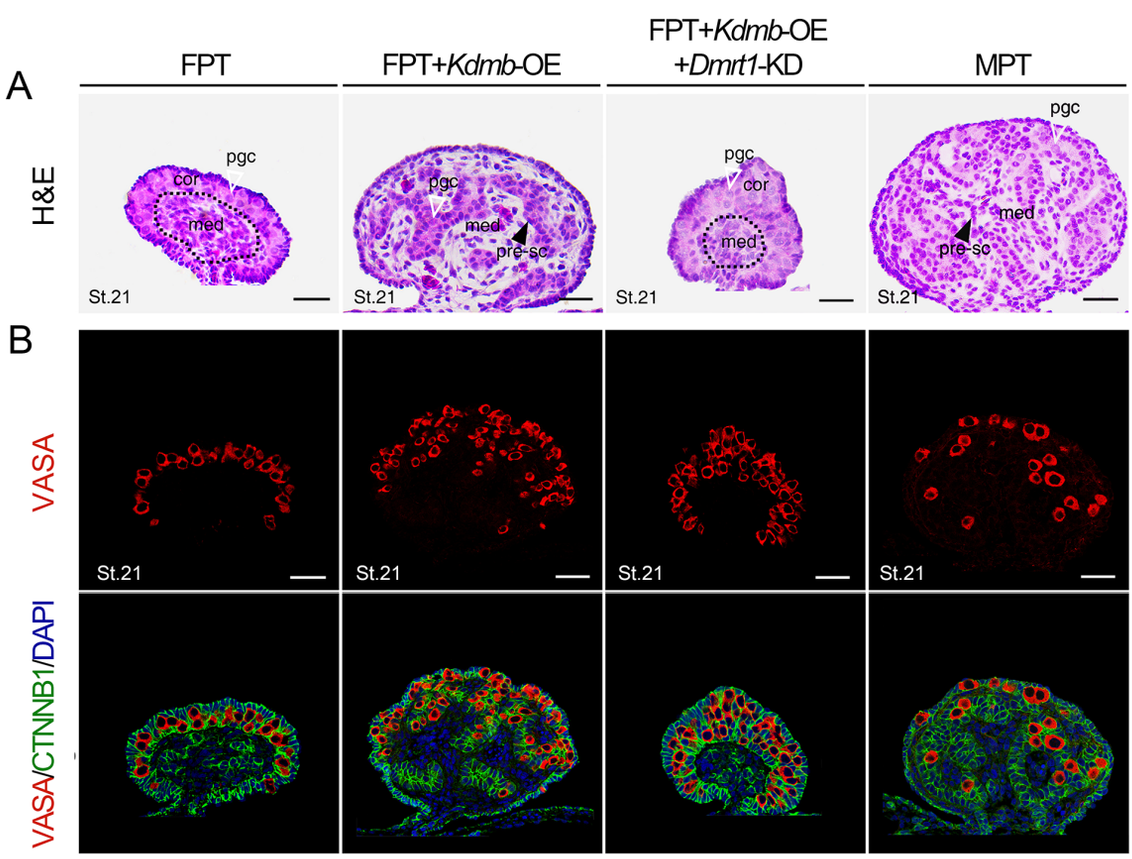

Figure 3 Restoration of gonadal structure and germ cell distribution in FPT gonads by *Dmrt1* knockdown after *Kdm6b* overexpression

A: H&E staining of gonadal sections from control FPT, FPT+*Kdm6b*-OE, FPT+*Kdm6b*-OE+*Dmrt1*-KD, and control MPT embryos at stage 21. Sc, seminiferous cord; pgc, primordial germ cells; cor, cortex; med, medulla. B: Immunofluorescence analysis of VASA and CTNNB1 proteins in gonadal sections from control FPT, FPT+*Kdm6b*-OE, FPT+*Kdm6b*-OE+*Dmrt1*-KD, and control MPT embryos at stage 21. VASA-positive germ cells were observed in the cortical region of FPT *Kdm6b*-OE+*Dmrt1*-KD gonads. Scale bars: 50 μm.

gonads (Figure 4A). Immunofluorescent staining confirmed the presence of the SOX9 protein in both the control MPT and *Kdm6b*-OE groups, but it was absent in both the control FPT and co-transduction group (Figure 4B). Notably, FOXL2 and CYP19A1 protein signals were detected in the co-transduction group (Figure 4C). Collectively, these findings provide strong evidence that *Dmrt1* functions downstream of *Kdm6b* to initiate the male developmental pathway in *T. s. elegans*.

DISCUSSION

We previously identified KDM6B as a key upstream regulator of the male developmental pathway, primarily through its role in catalyzing the demethylation of H3K27me3 near the *Dmrt1* promoter (Ge et al., 2017, 2018). Notably, we found that knockdown of *Kdm6b* under MPT conditions abolished *Dmrt1* expression and induced a male-to-female sex reversal, which could be rescued by *Dmrt1* overexpression. In the present study, we confirmed that overexpression of the *Kdm6b* ORF, driven by a cytomegalovirus (CMV) promoter, was sufficient for the induction of testicular development under FPT conditions. Additionally, co-injection with LV-*Dmrt1*-KD completely rescued the female phenotype. These findings underscore the role of *Kdm6b* as a predominant epigenetic regulator of *Dmrt1*, a critical gene for sex determination in turtles with a TSD system.

Accumulating evidence suggests that epigenetic regulation plays a pivotal role in sex determination across vertebrates, irrespective of whether the species follows GSD or TSD (Dupont & Capel, 2021; Garcia-Moreno et al., 2018; Weber & Capel, 2021). In particular, studies in mice have highlighted the involvement of various epigenetic readers, writers, and erasers —proteins that recognize, add, or remove post-translational modifications on histones —at the onset of sex determination, correlating with the maintenance, repression, and initiation of key genes essential for normal testicular development in XY males (Garcia-Moreno et al., 2019; Katoh-Fukui et al., 2012; Kuroki et al., 2013; Okashita et al., 2023). In *T. s. elegans*, although the specific epigenetic target differs, the mechanism by which KDM6B initiates *Dmrt1* expression is similar to the role of KDM3A in activating *Sry* in mice; both involve the removal of methyl tags from repressive histone marks to activate critical male pathway genes. Notably, *Kdm6b* and *Jarid2*, another Jumonji family member, are specifically expressed at lower temperatures in TSD species, including *T. s. elegans* and *Alligator mississippiensis* (Czerwinski et al., 2016; Deveson et al., 2017). While KDM6B functions as a demethylase, JARID2, a component of polycomb repressive complex 2 (PRC2), catalyzes the deposition of H3K27me3 at target loci (Sanulli et al., 2015). Given the rapid down-regulation of female-associated genes that coincides with the activation of the male pathway, it is plausible that KDM6B works as an eraser of H3K27me3 on *Dmrt1*, while JARID2 functions to suppress pro-ovarian factors, thereby reinforcing the male developmental pathway in turtles under MPT.

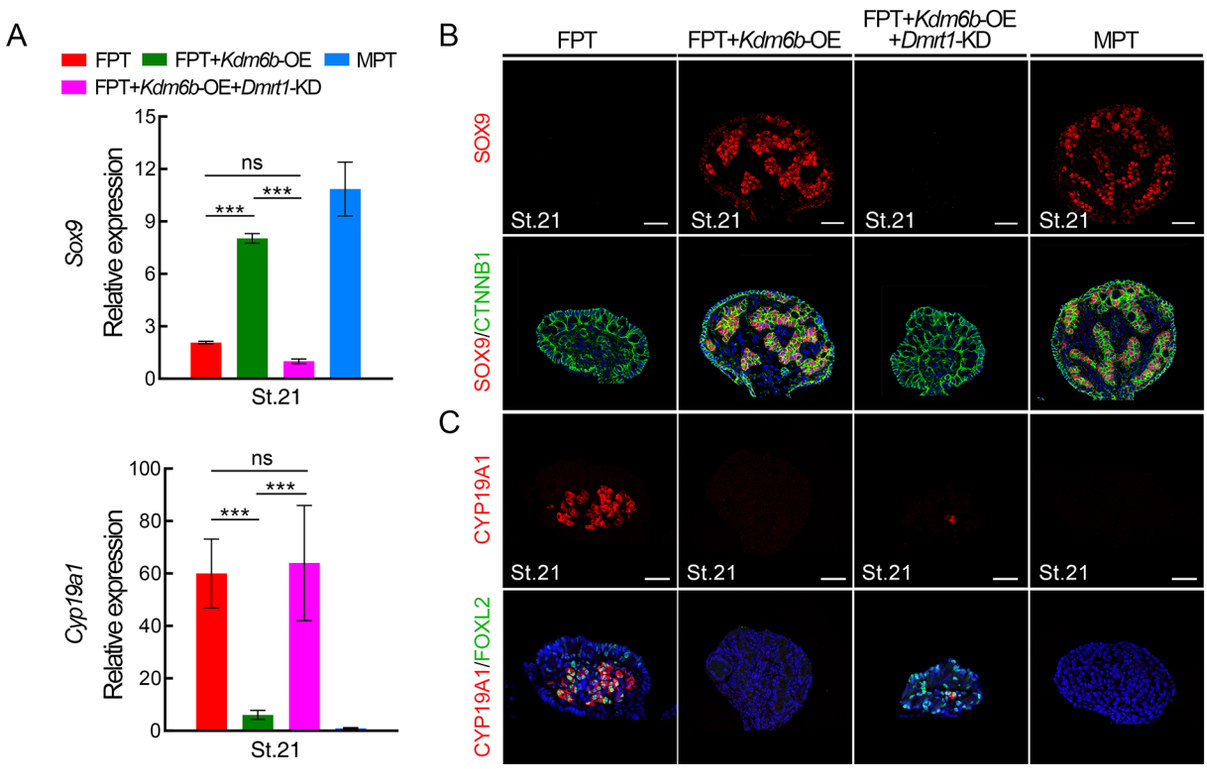

Figure 4 Masculinization of FPT gonads induced by *Kdm6b* overexpression can be reversed by knockdown of *Dmrt1*

A: mRNA expression of sex-specific markers in FPT gonads after *Kdm6b* overexpression and *Dmrt1* knockdown. Strong down-regulation of *Sox9* expression and significant up-regulation of *Cyp19a1* expression were observed in FPT *Kdm6b*-OE gonads following *Dmrt1* knockdown at stage 21. Results were normalized to *Gapdh*. Data are mean±SD; ***: P<0.001; ns: Not significant; n=3. B: Immunofluorescence staining of SOX9 and CTNNB1 proteins in gonadal sections from control FPT, FPT+*Kdm6b*-OE, FPT+*Kdm6b*-OE+*Dmrt1*-KD, and control MPT embryos at stage 21. Knockdown of *Dmrt1* following *Kdm6b* overexpression rescued female morphology and abolished SOX9 expression. C: Immunofluorescence staining of CYP19A1 and FOXL2 proteins in gonadal sections from control FPT, FPT+*Kdm6b*-OE, FPT+*Kdm6b*-OE+*Dmrt1*-KD, and control MPT embryos at stage 21. Knockdown of *Dmrt1* following *Kdm6b* overexpression rescued CYP19A1 and FOXL2 expression. Scale bars: 50 μm.

According to our results, *Kdm6b* plays a critical role in promoting male development in the TSD system. However, its function is context-dependent across different species. For instance, while low temperatures induce male development in *T. s. elegans*, they result in female offspring in *Alligator mississippiensis* (Yatsu et al., 2016). Additionally, in the Australian central bearded dragon (*Pogona vitticeps*), higher incubation temperatures induce male-to-female sex reversal in *ZZ* individuals, accompanied by an increase in *Kdm6b* expression (Deveson et al., 2017). These observations suggest that temperature does not directly regulate *Kdm6b* expression, nor does *Kdm6b* directly regulate sex differentiation. Instead, *Kdm6b* appears to function as an intermediary regulator, integrating temperature cues with the sex determination process in TSD animals. The consistent presence of sexually dimorphic *Kdm6b* expression across various TSD and temperature-induced sex reversal (TISR) species (Deveson et al., 2017; Whiteley et al., 2022; Yao et al., 2023) raises the question of how this epigenetic factor remains so conserved, especially given the high variability in its upstream and downstream regulatory networks among species.

Furthermore, alternative splicing has emerged as a significant mechanism in the regulation of sex determination (Casper & Van Doren, 2006; Gómez-Redondo et al., 2021). In particular, intron retention events in *Kdm6b* and *Jarid2* that produce C-terminal truncated transcripts are more prevalent at lower temperatures across different reptile species (Deveson et al., 2017; Whiteley et al., 2022), suggesting a potential role for alternative splicing in TSD. In our study, overexpression of the full-length *Kdm6b* ORF alone was sufficient to trigger a high rate of female-to-male sex reversal under FPT conditions, supporting the view that full-length *Kdm6b* is the dominant epigenetic regulator of male developmental pathway in *T. s. elegans*. A recent study in *Nile tilapia* similarly found that only the full-length *kdm6bb*, not the intron-retaining transcript, induced female-to-male sex reversal in XX individuals. This suggests that the expression of full-length *Kdm6bb* may be influenced by the frequency of intron retention events, with higher intron retention correlating with fewer full-length transcripts (Yao et al., 2023). However, in *T. s. elegans*, both intron-retaining and full-length transcripts were simultaneously up-regulated under MPT conditions, implying a different mechanism for this species (Deveson et al., 2017; Ge et al., 2018). Further research is needed to elucidate the role of C-terminal truncated *Kdm6b* transcripts in turtle sex determination.

Another important question is how does *Kdm6b* respond to temperature cues if it is not directly responsive to temperature? Our investigation into the upstream factors of *Kdm6b* identified a calcium-pSTAT3-*Kdm6b* signaling pathway that influences sex determination in turtles (Weber et al., 2020). However, the broader regulatory network remains largely unresolved. For example, the potential roles of transient receptor potential cation channels, calcium/calmodulin-dependent protein kinase II (CAMKII), cold-inducible RNA-binding protein (CIRBP)-induced JAK/STAT, and pressure-induced Src/STAT in this pathway are yet to be clarified (Hulsurkar et al., 2018; Sun et al., 2018; Vangeel & Voets, 2019; Wang et al., 2015). Thus, further evidence is essential to fully elucidate the complexities of TSD.

SUPPLEMENTARY DATA

Supplementary data to this article can be found online.

COMPETING INTERESTS

The authors declare that they have no competing interests.

AUTHORS' CONTRIBUTIONS

Q.C., W.S., and C.G. conceived and designed the study; Q.C., W.S., L.J., Y.Z., F.L., and C.G. performed the experiments and data analysis; Q.C., W.S., Y.Z., and C.G. designed the charts and tables. Q.C., W.S., and L.J. wrote the original manuscript; Q.C., F.L., and C.G. reviewed and edited the manuscript; All authors read and approved the final version of the manuscript.

ACKNOWLEDGMENTS

We thank members of the Ge laboratory for their support.

REFERENCES

Bertho S, Pasquier J, Pan QW, et al. 2016. Foxl2 and its relatives are evolutionary conserved players in gonadal sex differentiation. *Sexual Development*, **10**(3): 111–129.

Bull JJ, Vogt RC. 1979. Temperature-dependent sex determination in turtles. *Science*, **206**(4423): 1186–1188.

Casper A, Van Doren M. 2006. The control of sexual identity in the *Drosophila* germline. *Development*, **133**(15): 2783–2791.

Cutting A, Chue J, Smith CA. 2013. Just how conserved is vertebrate sex determination?. *Developmental Dynamics*, **242**(4): 380–387.

Czerwinski M, Natarajan A, Barske L, et al. 2016. A timecourse analysis of systemic and gonadal effects of temperature on sexual development of the red-eared slider turtle *Trachemys scripta elegans*. *Developmental Biology*, **420**(1): 166–177.

Deveson IW, Holleley CE, Blackburn J, et al. 2017. Differential intron retention in *Jumonji* chromatin modifier genes is implicated in reptile temperature-dependent sex determination. *Science Advances*, **3**(6): e1700731.

Dupont S, Capel B. 2021. The chromatin state during gonadal sex determination. *Sexual Development*, **15**(5-6): 308–316.

Garcia-Moreno SA, Lin YT, Futtner CR, et al. 2019. CBX2 is required to stabilize the testis pathway by repressing Wnt signaling. *PLoS Genetics*, **15**(5): e1007895.

Garcia-Moreno SA, Plebanek MP, Capel B. 2018. Epigenetic regulation of male fate commitment from an initially bipotential system. *Molecular and Cellular Endocrinology*, **468**: 19–30.

Ge CT, Ye J, Weber C, et al. 2018. The histone demethylase KDM6B regulates temperature-dependent sex determination in a turtle species. *Science*, **360**(6389): 645–648.

Ge CT, Ye J, Zhang HY, et al. 2017. *Dmrt1* induces the male pathway in a turtle species with temperature-dependent sex determination. *Development*, **144**(12): 2222–2233.

Gómez-Redondo I, Planells B, Navarrete P, et al. 2021. Role of alternative splicing in sex determination in vertebrates. *Sexual Development*, **15**(5-6): 381–391.

Greenbaum E, Carr JL. 2002. Staging criteria for embryos of the spiny softshell turtle, *Apalone spinifera* (Testudines: Trionychidae). *Journal of Morphology*, **254**(3): 272–291.

Hui HB, Xiao L, Sun W, et al. 2021. *Sox9* is indispensable for testis differentiation in the red-eared slider turtle, a reptile with temperature-dependent sex determination. *Zoological Research*, **42**(6): 721–725.

Hulsurkar M, Quick AP, Wehrens XH. 2018. STAT3: a link between CaMKII-β_{IV}-spectrin and maladaptive remodeling?. *Journal of Clinical Investigation*, **128**(12): 5219–5221.

Kashimada K, Koopman P. 2010. *Sry*: the master switch in mammalian sex

determination. *Development*, **137**(23): 3921–3930.

Katoh-Fukui Y, Miyabayashi K, Komatsu T, et al. 2012. *Cbx2*, a polycomb group gene, is required for *Sry* gene expression in mice. *Endocrinology*, **153**(2): 913–924.

Koopman P, Gubbay J, Vivian N, et al. 1991. Male development of chromosomally female mice transgenic for *Sry*. *Nature*, **351**(6322): 117–121.

Kuroki S, Matoba S, Akiyoshi M, et al. 2013. Epigenetic regulation of mouse sex determination by the histone demethylase jmjd1a. *Science*, **341**(6150): 1106–1109.

Kuroki S, Tachibana M. 2018. Epigenetic regulation of mammalian sex determination. *Molecular and Cellular Endocrinology*, **468**: 31–38.

Ma XH, Liu F, Chen QR, et al. 2022. *Foxl2* is required for the initiation of the female pathway in a temperature-dependent sex determination system in *Trachemys scripta*. *Development*, **149**(13): dev200863.

Matsumoto Y, Buemio A, Chu R, et al. 2013. Epigenetic control of gonadal aromatase (*cyp19a1*) in temperature-dependent sex determination of red-eared slider turtles. *PLoS One*, **8**(6): e63599.

Okashita N, Maeda R, Tachibana M. 2023. CDYL reinforces male gonadal sex determination through epigenetically repressing *Wnt4* transcription in mice. *Proceedings of the National Academy of Sciences of the United States of America*, **120**(20): e2221499120.

Reik W. 2007. Stability and flexibility of epigenetic gene regulation in mammalian development. *Nature*, **447**(7143): 425–432.

Sanulli S, Justin N, Teissandier A, et al. 2015. Jarid2 methylation via the PRC2 complex regulates H3K27me3 deposition during cell differentiation. *Molecular Cell*, **57**(5): 769–783.

Schwanz LE, Georges A. 2021. Sexual development and the environment: conclusions from 40 years of theory. *Sexual Development*, **15**(1-3): 7–22.

Shao CW, Li QY, Chen SL, et al. 2014. Epigenetic modification and inheritance in sexual reversal of fish. *Genome Research*, **24**(4): 604–615.

Smith CA, Roeszler KN, Ohnesorg T, et al. 2009. The avian Z-linked gene *DMRT1* is required for male sex determination in the chicken. *Nature*, **461**(7261): 267–271.

Sun WC, Liao Y, Yi Q, et al. 2018. The mechanism of CIRP in regulation of STAT3 phosphorylation and Bag-1/S expression upon UVB radiation. *Photochemistry and Photobiology*, **94**(6): 1234–1239.

Tezak B, Straková B, Fullard DJ, et al. 2023. Higher temperatures directly increase germ cell number, promoting feminization of red-eared slider turtles. *Current Biology*, **33**(14): 3017–3023. e2.

Vangeel L, Voets T. 2019. Transient receptor potential channels and calcium signaling. *Cold Spring Harbor Perspectives in Biology*, **11**(6): a035048.

Vining B, Ming ZH, Bagheri-Fam S, et al. 2021. Diverse regulation but conserved function: SOX9 in vertebrate sex determination. *Genes*, **12**(4): 486.

Wang L, Sun F, Wan ZY, et al. 2022. Transposon-induced epigenetic silencing in the X chromosome as a novel form of *dmrt1* expression regulation during sex determination in the fighting fish. *BMC Biology*, **20**(1): 5.

Wang WS, Guo CM, Zhu P, et al. 2015. Phosphorylation of STAT3 mediates the induction of cyclooxygenase-2 by cortisol in the human amnion at parturition. *Science Signaling*, **8**(400): ra106.

Warner DA, Shine R. 2008. The adaptive significance of temperature-dependent sex determination in a reptile. *Nature*, **451**(7178): 566–568.

Weber C, Capel B. 2021. Sex determination without sex chromosomes. *Philosophical Transactions of the Royal Society B: Biological Sciences*, **376**(1832): 20200109.

Weber C, Zhou YJ, Lee JG, et al. 2020. Temperature-dependent sex determination is mediated by pSTAT3 repression of *Kdm6b*. *Science*, **368**(6488): 303–306.

Wei A, Wu H. 2022. Mammalian DNA methylome dynamics: mechanisms, functions and new frontiers. *Development*, **149**(24): dev182683.

Whiteley SL, Wagner S, Holleley CE, et al. 2022. Truncated *jarid2* and *kdm6b* transcripts are associated with temperature-induced sex reversal during development in a dragon lizard. *Science Advances*, **8**(16): eabk0275.

Wibbels T, Bull JJ, Crews D. 1991. Chronology and morphology of temperature-dependent sex determination. *Journal of Experimental Zoology*, **260**(3): 371–381.

Yao ZL, Fang QF, Li JY, et al. 2023. Alternative splicing of histone demethylase *Kdm6bb* mediates temperature-induced sex reversal in the Nile tilapia. *Current Biology*, **33**(23): 5057–5070. e5.

Yatsu R, Miyagawa S, Kohno S, et al. 2016. RNA-seq analysis of the gonadal transcriptome during *Alligator mississippiensis* temperature-dependent sex determination and differentiation. *BMC Genomics*, **17**: 77.